

# Analysis of Near-Field Effects of Wave Field Synthesis using Linear Loudspeaker Arrays

Sascha Spors and Jens Ahrens

<sup>1</sup>*Deutsche Telekom Laboratories, Ernst-Reuter-Platz 7, 10587 Berlin, Germany*

Correspondence should be addressed to Sascha Spors (Sascha.Spors@telekom.de)

## ABSTRACT

Wave field synthesis (WFS) is a technique allowing the reproduction of sound fields in an extended listening area. This paper describes the theoretical fundamentals of WFS using linear loudspeaker arrays. A spatio-temporal frequency domain analysis of the reproduced wave field reveals that not only the desired wave field is present in the listening area but also an additional near-field component. This component is analyzed in detail and the resulting wave fields are illustrated. Practical realizations of WFS impose certain technical constraints, namely the application of a finite number of discrete loudspeakers. The impact of this spatial discretization and truncation of the secondary source distribution on the near-field component is derived.

## 1. INTRODUCTION

Spatial sound reproduction systems with a high number of loudspeakers (massive multichannel sound reproduction systems) have increasingly been used in the last decade. The use of more and more loudspeakers has increased the reproduction quality considerably in the past. However, most systems still suffer from several artifacts present in the reproduced wave field. This contribution discusses one of these artifacts, namely near-field effects of linear arrays where each loudspeaker is realized by a line array.

Typical sound reproduction systems aim at reproducing the wave field at the level of the listeners ears only. Hence a two-dimensional formulation of sound reproduction is suitable for most applications and will be applied in this paper. The presented principles can be generalized straightforwardly to three-dimensional reproduction.

One of the reproduction systems proposed in the context of massive multichannel systems is wave field synthesis (WFS). It is intuitively based on the Huygens principle or more mathematically on the Kirchhoff-Helmholtz integral [1, 2]. Previous studies [3, 4] of the wave field reproduced by a WFS system using a linear loudspeaker array revealed that there are additional artifacts reproduced besides the desired wave field of the virtual source. However, to the knowledge of the authors these artifacts have not been analyzed for WFS in detail up to now. This paper complements this finding by suggesting that these additional contributions are near-field effects of the loud-

speaker array.

This paper proceeds as follows: First the theoretical background of WFS is introduced in Section 2, then a detailed analysis of the near-field effects is given in Section 3. This is followed by a generalization of the results to point sources as secondary sources in Section 4. Finally, Section 5 gives a short summary, some conclusions and an outlook on further research directions.

### 1.1. Nomenclature

The following conventions are used throughout this paper: For scalar variables lower case denotes the time domain, upper case the temporal frequency domain. Vectors are denoted by lower case boldface. The spatial frequency domain is denoted by a tilde placed over the respective symbol. The two-dimensional position vector in Cartesian coordinates is given as  $\mathbf{x} = [x \ y]^T$ . The analysis is performed entirely in the temporal frequency domain by transforming all signals and wave fields from the time domain into the frequency domain by a (temporal) Fourier transformation [5]. The temporal frequency variable is denoted by  $\omega = 2\pi f$ .

## 2. WAVE FIELD SYNTHESIS

The following section provides the fundamentals of sound reproduction and WFS as required within this paper. For more details please refer to [6, 7, 1, 2].

### 2.1. Fundamentals of sound reproduction

The theoretical basis of most loudspeaker-based sound reproduction systems is given by the Kirchhoff-

Helmholtz integral [8]. It states, that the acoustic pressure inside a closed region  $V$  can be controlled by a continuous monopole and dipole source distribution on the boundary  $\partial V$  enclosing the region  $V$ . These sources are termed as *secondary sources* in the following. The wave field to be reproduced will be denoted as *virtual source* wave field.

It is desirable to remove the secondary dipole sources for a practical realization of spatial sound reproduction systems. The reproduced wave field for monopole-only reproduction is given as [6, 7]

$$P(\mathbf{x}, \omega) = - \oint_{\partial V} \underbrace{2a(\mathbf{x}_0) \frac{\partial}{\partial \mathbf{n}} S(\mathbf{x}_0, \omega)}_{D(\mathbf{x}_0, \omega)} G(\mathbf{x}|\mathbf{x}_0, \omega) dS_0, \quad (1)$$

where  $S(\mathbf{x}_0, \omega)$  denotes the wave field of the virtual source at the boundary  $\partial V$ ,  $a(\mathbf{x}_0)$  a window function which determines which secondary sources are excited, and  $G(\mathbf{x}|\mathbf{x}_0, \omega)$  a suitably chosen free-field Green's function representing the secondary sources. The operator  $\frac{\partial}{\partial \mathbf{n}}$  denotes the gradient in direction of the inward pointing surface normal  $\mathbf{n}$ . A relevant secondary source, in this context, is a source whose propagation direction coincides with the local wave field of the virtual source. The secondary source driving function  $D(\mathbf{x}_0, \omega)$  abbreviates the terms constituting the strength of the secondary sources.

For two-dimensional sound reproduction the required Green's function is given by the two-dimensional free-field Green's function

$$G_{2D}(\mathbf{x}|\mathbf{x}_0, \omega) = \frac{j}{4} H_0^{(2)}(k|\mathbf{x} - \mathbf{x}_0|), \quad (2)$$

where  $H_0^{(2)}(\cdot)$  denotes the zeroth order Hankel function of second kind and  $k = \omega/c$  the wave number. The physical interpretation of  $G_{2D}(\mathbf{x}, \omega)$ , in three-dimensional space, is the wave field produced by a line source. A practical realization of a line source is a line array. The three-dimensional free-field Green's function is required for three-dimensional reproduction. It is given as

$$G_{3D}(\mathbf{x}|\mathbf{x}_0, \omega) = \frac{1}{4\pi} \frac{e^{-jk|\mathbf{x} - \mathbf{x}_0|}}{|\mathbf{x} - \mathbf{x}_0|}. \quad (3)$$

The physical interpretation of  $G_{3D}(\mathbf{x}, \omega)$  is the field produced by a point source. A practical realization of a point source is a loudspeaker with closed cabinet.

## 2.2. Wave Field Synthesis

Wave field synthesis is typically a two-dimensional spatial sound reproduction technique which uses loudspeakers with closed cabinets as secondary sources [7, 1, 2]. Closed loudspeakers can be regarded as approximations of point sources. The acoustical field of a point source is provided by the three-dimensional free-field Green's function  $G_{3D}(\mathbf{x}|\mathbf{x}_0, \omega)$ . However, line sources would be more appropriate as secondary sources for a two-dimensional sound reproduction system. In order to analyze and compensate the error introduced by this secondary source mismatch a closer look at the properties of point and line sources is taken. The asymptotic expansion of the Hankel function for large arguments [9] is used to approximate the two-dimensional Green's function  $G_{2D}(\mathbf{x}|\mathbf{x}_0, \omega)$  as follows

$$G_{2D}(\mathbf{x}|\mathbf{x}_0, \omega) \approx \frac{1}{4\pi} \sqrt{\frac{2\pi}{jk}} \frac{1}{\sqrt{|\mathbf{x} - \mathbf{x}_0|}} e^{-jk|\mathbf{x} - \mathbf{x}_0|}. \quad (4)$$

Comparing Eq. (4) with Eq. (3) reveals that the given approximation of  $G_{2D}(\mathbf{x}|\mathbf{x}_0, \omega)$  is similar to a point source but with a different spectrum and amplitude decay. This reveals that a frequency and amplitude correction can be applied in order to compensate for the secondary source mismatch. For WFS both corrections are typically included into the secondary source driving function  $D(\mathbf{x}_0, \omega)$ . In general, the amplitude can only be corrected exactly for one listener position in the listening area. For other positions, amplitude errors are present in the reproduced wave field [10, 11]. Note that the corrections outlined above assume that the large argument approximation ( $k|\mathbf{x} - \mathbf{x}_0| \gg 1$ ) holds.

## 2.3. Linear loudspeaker arrays

Practical implementations of WFS systems facilitate linear or circular loudspeaker arrays. We will focus on linear secondary line source distributions in this paper. Without loss of generality, the geometry depicted in Fig. 1 is assumed: a linear secondary source distribution located on the  $x$ -axis ( $y = 0$ ) of a Cartesian coordinate system. The reproduced wave field is derived from Eq. (1) by degenerating the closed contour  $\partial V$  to a line on the  $x$ -axis with infinite length. This line divides the  $xy$ -plane in two-regions. The upper half plane ( $y > 0$ ) is chosen as the listening area. Please note that for this specialized geometry only those virtual source wave fields can be reproduced where the local propagation direction at the secondary source distribution has a contribution in the direction of the positive  $y$ -axis. The window function

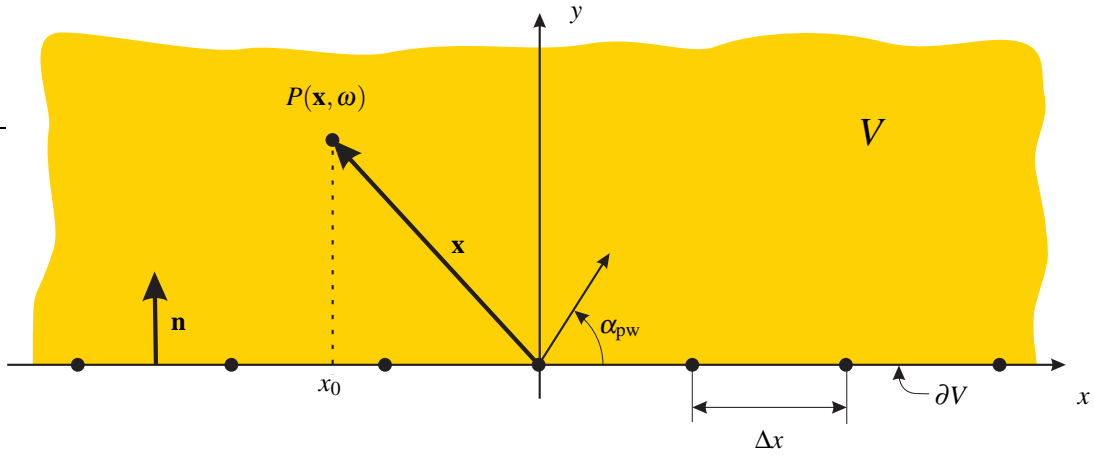


**Fig. 1:** Geometry used to derive the reproduced wave field of a linear secondary source distribution. The • denote the sampling positions of the secondary sources for a discontinuous secondary source distribution (loudspeaker array).

$a(\mathbf{x}_0) = 1$  in this case.

Specializing Eq. (1) to the geometry depicted by Fig. 1 yields

$$P(\mathbf{x}, \omega) = - \int_{-\infty}^{\infty} D(\mathbf{x}_0, \omega) G(\mathbf{x} - \mathbf{x}_0, \omega) dx_0, \quad (5)$$

where  $\mathbf{x}_0 = [x_0 \ 0]^T$  and  $G(\mathbf{x}|\mathbf{x}_0, \omega) = G(\mathbf{x} - \mathbf{x}_0, \omega)$  for typical Green's functions used in this context. The integral (5) is also known as Rayleigh integral [8].

The next section will derive the near-field effects for a linear secondary line source distribution.

### 3. NEAR-FIELD EFFECTS OF LINEAR LOUDSPEAKER ARRAYS

For the following analysis of the near-field effects of linear loudspeaker arrays the idealized case of secondary line sources will be assumed in order to discard the amplitude and spectral errors of WFS. The near-field effects of linear line arrays are derived by a spatio-temporal frequency domain analysis of the reproduced wave field. This analysis is based on the frequency domain representation published by one of the authors in [3, 4].

A monochromatic plane wave is assumed as the wave field of the virtual source  $S(\mathbf{x}_0, \omega)$  in the following. The derived results can be generalized straightforwardly, since arbitrary wave fields can be represented as the superposition of monochromatic plane waves [8, 6].

#### 3.1. Spatio-temporal frequency-domain representation of the reproduced wave field

The spatio-temporal frequency-domain representation

of the reproduced wave field is derived by applying a two-dimensional spatial Fourier transformation to the signals and wave fields given in the temporal frequency domain. The applied two-dimensional spatial Fourier transformation is defined as follows

$$\begin{aligned} \tilde{P}(\mathbf{k}, \omega) &= \mathcal{F}_{\mathbf{x}}\{P(\mathbf{x}, \omega)\} \\ &= \int_{-\infty}^{\infty} \int_{-\infty}^{\infty} P(\mathbf{x}, \omega) e^{-j\mathbf{k}^T \mathbf{x}} d\mathbf{x}, \end{aligned} \quad (6)$$

where the vector  $\mathbf{k} = [k_x \ k_y]^T$  denotes the spatial frequency vector (wave vector). It is related to the temporal frequency by  $|\mathbf{k}| = k = \omega/c$  for acoustic wave fields, where  $c$  denotes the speed of sound. Applying the two-dimensional spatial Fourier transformation (6) to Eq. (5) yields the spatio-temporal spectrum of the wave field reproduced by a linear secondary source distribution as

$$\tilde{P}(\mathbf{k}, \omega) = -\tilde{D}(k_x, \omega) \tilde{G}(\mathbf{k}, \omega). \quad (7)$$

In order to compute the reproduced spectrum, the spatio-temporal spectrums of the secondary line sources  $\tilde{G}_{2D}(\mathbf{k}, \omega)$  and the driving function  $\tilde{D}(k_x, \omega)$  have to be considered. Introducing the spectrum of the secondary line sources and the driving function for a plane wave into Eq. (7) yields the reproduced spectrum as [3]

$$\begin{aligned} \tilde{P}_{pw}(\mathbf{k}, \omega) &= \pi \frac{\omega}{c} \sin \alpha_{pw} \delta(k_x - \frac{\omega}{c} \cos \alpha_{pw}) \times \\ &\times \left( \frac{1}{k} \delta(\sqrt{k_x^2 + k_y^2} - \frac{\omega}{c}) + j \frac{1}{k_x^2 + k_y^2 - (\frac{\omega}{c})^2} \right). \end{aligned} \quad (8)$$

The reproduced spectrum consists of a real and an imaginary valued part. Throughout this paper these will be denoted as follows

$$\tilde{P}_{pw}(\mathbf{k}, \omega) = \underbrace{\Re\{\tilde{P}_{pw}(\mathbf{k}, \omega)\}}_{\tilde{P}_{pw,pr}(\mathbf{k}, \omega)} + j \underbrace{\Im\{\tilde{P}_{pw}(\mathbf{k}, \omega)\}}_{\tilde{P}_{pw,ev}(\mathbf{k}, \omega)}. \quad (9)$$

We will first analyze the real part in detail.

Applying the sifting property of the Dirac function to the real part  $\tilde{P}_{pw,pr}(\mathbf{k}, \omega)$  and rearranging the argument of the second (circular) Dirac line yields the following alternative form for  $\tilde{P}_{pw,pr}(\mathbf{k}, \omega)$

$$\tilde{P}_{pw,pr}(\mathbf{k}, \omega) = \pi \delta(k_x - \frac{\omega}{c} \cos \alpha_{pw}) \delta(k_y \pm \frac{\omega}{c} \sin \alpha_{pw}). \quad (10)$$

Inverse spatial Fourier transformation of  $\tilde{P}_{pw,pr}(\mathbf{k}, \omega)$  yields for  $y \geq 0$

$$P_{pw,pr}(\mathbf{x}, \omega) = \frac{1}{4\pi} e^{-j\mathbf{k}_{pw}^T \mathbf{x}}, \quad (11)$$

where

$$\mathbf{k}_{pw} = [k_{x,pw} \quad k_{y,pw}]^T \\ = [k \cos \alpha_{pw} \quad k \sin \alpha_{pw}]^T. \quad (12)$$

Inspection of  $P_{pw,pr}(\mathbf{x}, \omega)$  reveals that the real part of the spectrum of the reproduced wave field constitutes the desired plane wave. It propagates into the direction of the positive y-axis with the incidence angle  $\alpha_{pw}$ . This contribution is therefore termed as *propagating* part.

The reproduced spectrum  $\tilde{P}_{pw}(\mathbf{k}, \omega)$ , however, consists also of the additive imaginary valued part  $\tilde{P}_{pw,ev}(\mathbf{k}, \omega)$  besides the real part identified as the desired plane wave. The question arises what influence this part has on the field reproduced by a sound reproduction system. It will be derived in the following sections that this part can be identified as the near-field contribution.

### 3.2. Identification of near-field contributions

The inverse spatial Fourier transformation of the imaginary valued part  $\tilde{P}_{pw,ev}(\mathbf{k}, \omega)$  of the spectrum of the reproduced wave field is calculated in order to derive an interpretation of this part. The inverse Fourier transformation of  $\tilde{P}_{pw,ev}(\mathbf{k}, \omega)$  for  $y \geq 0$  is given as [12, Eq. 3.354-5]

$$P_{pw,ev}(\mathbf{x}, \omega) = \frac{1}{4\pi} e^{-jk_{x,pw}x} e^{-k_{y,pw}y}, \quad (13)$$

where  $k_{x,pw}$  and  $k_{y,pw}$  are defined according to Eq. (12). The field  $P_{pw,ev}(\mathbf{x}, \omega)$  exhibits the form of a two-dimensional evanescent plane wave [8].

Evanescent plane waves are solutions of the wave equation in the form of plane waves, where one of the elements of the wave vector  $\mathbf{k}_{pw}$  is imaginary. The amplitude of the evanescent wave decays exponentially in this direction, as a consequence. Evanescent waves can be observed in problems involving e. g. vibrating plates or wave reflection and transmission between two different media. They are also termed as near-field of a source due to their local structure given by the exponential decay of amplitude.

The evanescent plane wave  $P_{pw,ev}(\mathbf{x}, \omega)$  generated by the linear secondary source distribution oscillates parallel to the x-direction and its amplitude decays exponentially in the y-direction. The wavenumber of the oscillation in the x-direction is similar to the wavenumber  $k_{x,pw}$  of the desired plane wave in this direction, the exponent of the decay in the y-direction is proportional to the wavenumber  $k_{y,pw}$  of the desired plane wave in the y-direction. Using results from [8] it can be derived that the power flow is parallel to the x-axis, decaying exponentially in the y-direction.

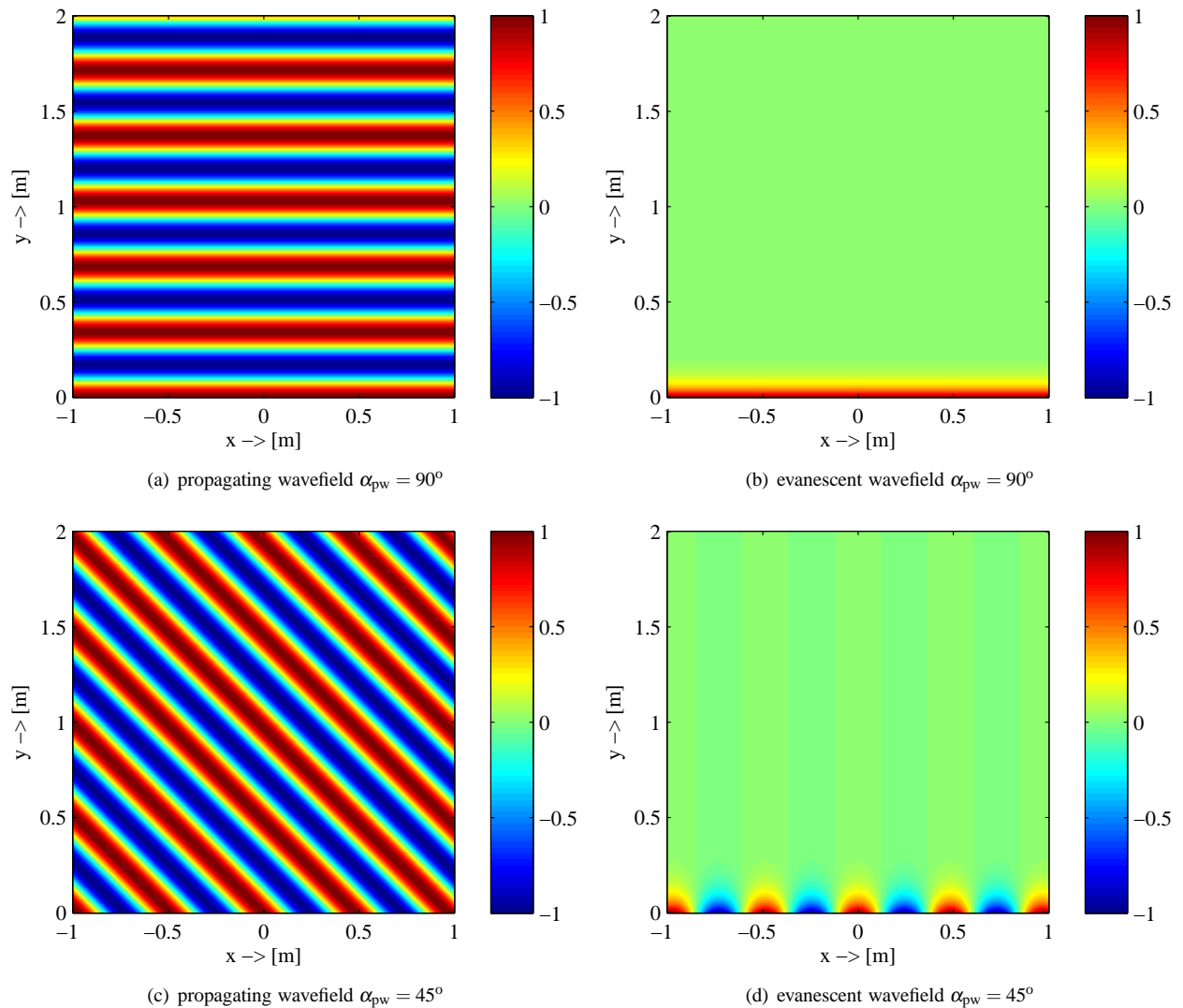
Figure 2 shows the propagating  $P_{pw,pr}(\mathbf{x}, \omega)$  and evanescent parts  $P_{pw,ev}(\mathbf{x}, \omega)$  of the wave field reproduced by a continuous linear secondary source distribution. The reproduced wave field for the desired reproduction of a monochromatic plane wave with frequency  $f = 1000$  Hz and two different incidence angles  $\alpha_{pw} = \{45^\circ, 90^\circ\}$  is shown. Note that the amplitude of the wave fields has been normalized by discarding the  $1/4\pi$  factor present in both fields.

Figure 3 illustrates the amplitude decay of the evanescent part along the y-axis for two different frequencies and incidence angles. The dependence on these variables can be seen clearly. It is also evident that the amplitude of the evanescent part of the reproduced wave field at some fixed distance from the array is higher for lower frequencies and incidence angles  $\alpha_{pw}$  different from 90 degrees.

### 3.3. Spatial sampling of continuous secondary source distributions

Practical implementations of sound reproduction and WFS systems utilize loudspeakers placed at discrete positions. The influence of this spatial sampling of the secondary source distribution on the reproduced wave field will be investigated in the following.

The reproduced spectrum  $\tilde{P}_{S,pw}(\mathbf{k}, \omega)$  for a discontinuous secondary line source distribution has been derived



**Fig. 2:** Propagating  $P_{pw,pr}(\mathbf{x}, \omega)$  and evanescent part  $P_{pw,ev}(\mathbf{x}, \omega)$  of the wave field reproduced by a continuous linear secondary source distribution for the reproduction of a plane wave with frequency  $f = 1000$  Hz and two different incidence angles  $\alpha_{pw}$ . The reproduced wave field is given as the superposition of both contributions.

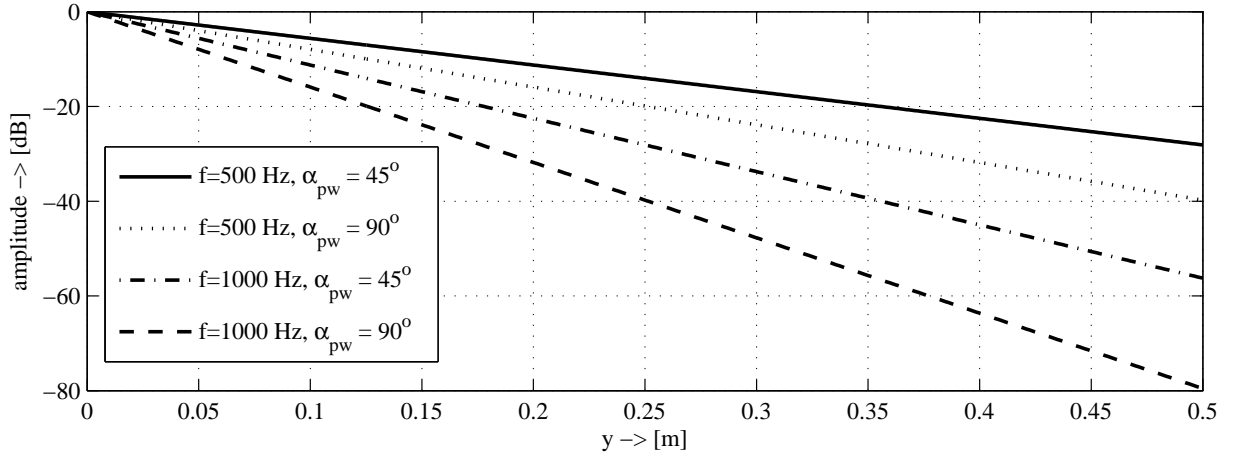


**Fig. 3:** Illustration of the amplitude decay of the evanescent part for two different frequencies  $f = \{500, 1000\}$  Hz and incidence angles  $\alpha_{pw} = \{45^\circ, 90^\circ\}$ .

in [3]. It is given as

$$\begin{aligned} \tilde{P}_{S,pw}(\mathbf{k}, \omega) = & \pi \frac{\omega}{c} \sin \alpha_{pw} \sum_{\eta=-\infty}^{\infty} \delta(k_x - \frac{2\pi}{\Delta x} \eta - \frac{\omega}{c} \cos \alpha_{pw}) \times \\ & \times \left( \frac{1}{k} \delta(\sqrt{k_x^2 + k_y^2} - \frac{\omega}{c}) + j \frac{1}{k_x^2 + k_y^2 - (\frac{\omega}{c})^2} \right), \quad (14) \end{aligned}$$

where  $\Delta x$  denotes the distance between the secondary sources (see Fig. 1), the index  $S$  indicates a sampled secondary source distribution. Spatial sampling leads to additional propagating plane waves in the reproduced wave field. The effect of spatial sampling on the propagating part and anti-aliasing conditions have already been discussed in [3, 4]. In this contribution we will focus on the effects of spatial sampling on the near-field contributions.

The reproduced wave field  $\tilde{P}_{S,pw}(\mathbf{k}, \omega)$  is split into a real and an imaginary valued part, according to Eq. (9). Figure 4 illustrates the structure of the imaginary valued part  $\tilde{P}_{S,pw,ev}(\mathbf{k}, \omega)$  of the reproduced spectrum in the spatial frequency domain. This part consists of a series of Dirac lines parallel to the  $k_x$ -axis weighted by a contribution which is inversely proportional to  $k_x^2 + k_y^2 - (\frac{\omega}{c})^2$ . The poles of this weighting contribution lie on a circle with radius  $\omega/c$ , the values are negative inside the circle and positive outside. No exact anti-aliasing condition can be derived for the imaginary valued part since the weighting of the Dirac lines never becomes zero. As a consequence,

aliasing artifacts will always be present in the near-field contributions of the reproduced wave field. However, this is not the case for the propagating part of the reproduced wave field.

Inverse spatial Fourier transformation of the imaginary valued part  $\tilde{P}_{S,pw,ev}(\mathbf{k}, \omega)$  using [12, Eq. 3.354-5] for  $y > 0$  yields

$$\begin{aligned} P_{S,pw,ev}(\mathbf{x}, \omega) = & \frac{j\omega}{4c} \sin \alpha_{pw} \times \\ & \times \sum_{\eta=-\infty}^{\infty} e^{-j(\frac{2\pi}{\Delta x} \eta + \frac{\omega}{c} \cos \alpha_{pw})x} \frac{1}{a_\eta} e^{-|a_\eta y|}, \quad (15) \end{aligned}$$

where  $a_\eta$  is given as

$$a_\eta^2 = \left( \frac{2\pi}{\Delta x} \eta + \frac{\omega}{c} \cos \alpha_{pw} \right)^2 - \left( \frac{\omega}{c} \right)^2. \quad (16)$$

Please note that Eq. (15) is equal to Eq. (13) for  $\eta = 0$ . The inverse Fourier transformation of the imaginary valued part  $P_{S,pw,ev}(\mathbf{x}, \omega)$  for a sampled secondary line source distribution consists of a superposition of evanescent plane waves. The wavenumber of the oscillating part in the  $x$ -direction is given by the wavenumber of the desired plane wave in the  $x$ -direction and its repetitions at  $\frac{2\pi}{\Delta x} \eta$  due to the spatial sampling. The exponent of the decay in the  $y$ -direction is proportional to the factor  $a_\eta$ . The factor  $a_\eta$  given by Eq. (16) can be interpreted as the cathetus of a right angled triangle, as shown in Fig. 4 for  $a_1$ . Hence,  $a_\eta$  is imaginary for all  $\eta$  were the Dirac

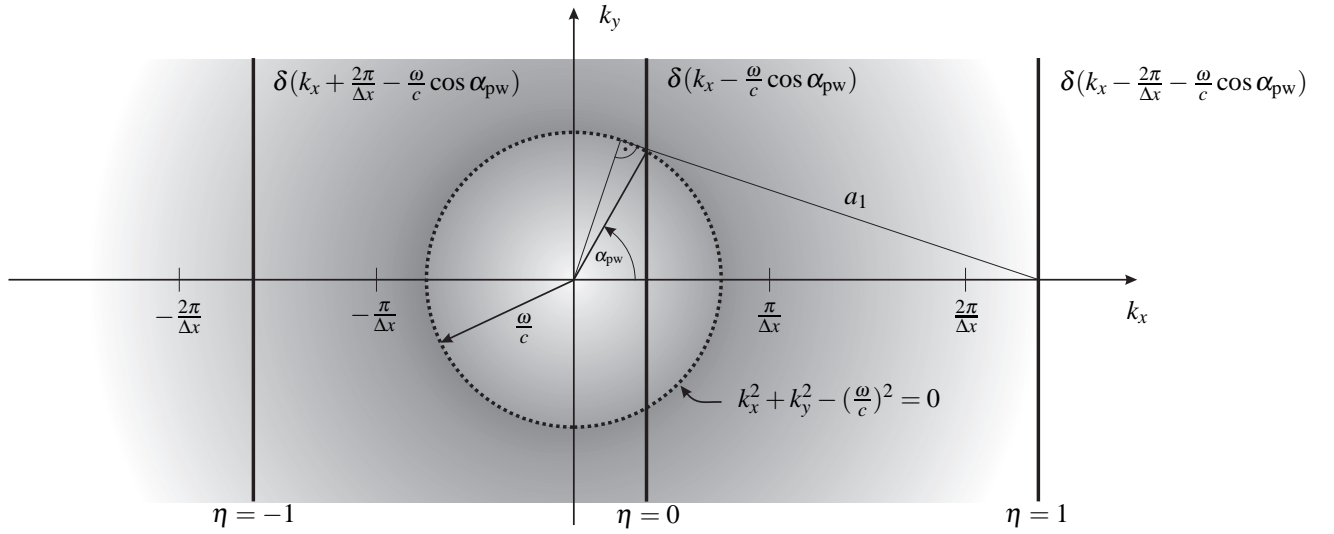


**Fig. 4:** Illustration of the imaginary valued part of the reproduced spectrum  $\tilde{P}_{S,pw}$  by a discrete secondary line source distribution for the reproduction of a plane wave with incidence angle  $\alpha_{pw}$ .

lines intersect with the circular pole and real otherwise. Please note, that additional Dirac lines intersect with the circular pole in Fig. 4 if the frequency of the monochromatic plane wave or the secondary source distance  $\Delta x$  is increased.

For the  $x$ -axis ( $y = 0$ ) Eq. (15) can be rewritten as a Fourier series with respect to the  $x$ -coordinate

$$P_{S,pw,ev}(x, 0, \omega) = \frac{j\omega}{4c} \sin \alpha_{pw} \times \frac{1}{\Delta x} e^{-j\frac{\omega}{c} \cos \alpha_{pw} x} \sum_{\eta=-\infty}^{\infty} \frac{1}{a_{\eta}} e^{-j\frac{2\pi}{\Delta x} \eta x}. \quad (17)$$

Hence, the factors  $\frac{1}{a_{\eta}}$  can be regarded as the Fourier series coefficients of the reproduced field on the  $x$ -axis.

Figure 5 shows the evanescent part of the wave field reproduced by a continuous and a sampled secondary source distribution. Again the reproduction of a plane wave with a frequency of  $f = 1000$  Hz and incidence angle  $\alpha_{pw} = 45^\circ$  is considered. The secondary source distance was chosen to be  $\Delta x = 10$  cm. This way no spatial sampling artifacts will be present in the reproduced propagating part [4]. Figure 5(a) is a zoomed version of Fig. 2(d) to allow a better visualization of the decaying evanescent part. Please note that the amplitude of the wave fields has been normalized. The aliasing artifacts for the evanescent part are clearly visible in Fig. 5(b).

### 3.4. Truncated linear arrays

Up to now, the linear secondary source distribution was assumed to be of infinite length in the  $x$ -direction. However, practical implementations of linear loudspeaker arrays will always be of finite length. In [3] truncation of a linear secondary source distribution was only discussed on a qualitative level by considering a limited reproduction area. The limitation is based on a geometric approximation of the truncation effects. This approximation states that a plane wave will only be reproduced in a tilted rectangular area in front of the array, whose width is equivalent to the aperture of the array in the  $x$ -direction and whose length in the  $y$ -direction is infinite. The area is tilted by the incidence angle  $\alpha_{pw}$  of the plane wave to be reproduced.

We will now give some details on the quantitative description of the truncation effects. Truncation is typically modeled by multiplying the secondary source driving function  $D(x_0, \omega)$  with a suitable window function  $w(x_0)$  [1]. Incorporating  $w(x_0)$  into Eq. (5) yields the wave field  $P_{tr}(\mathbf{x}, \omega)$  reproduced by a truncated linear array as

$$P_{tr}(\mathbf{x}, \omega) = - \int_{-\infty}^{\infty} w(x_0) D(\mathbf{x}_0, \omega) G(\mathbf{x} - \mathbf{x}_0, \omega) dx_0. \quad (18)$$

Spatial Fourier transformation of  $P_{tr}(\mathbf{x}, \omega)$  yields the

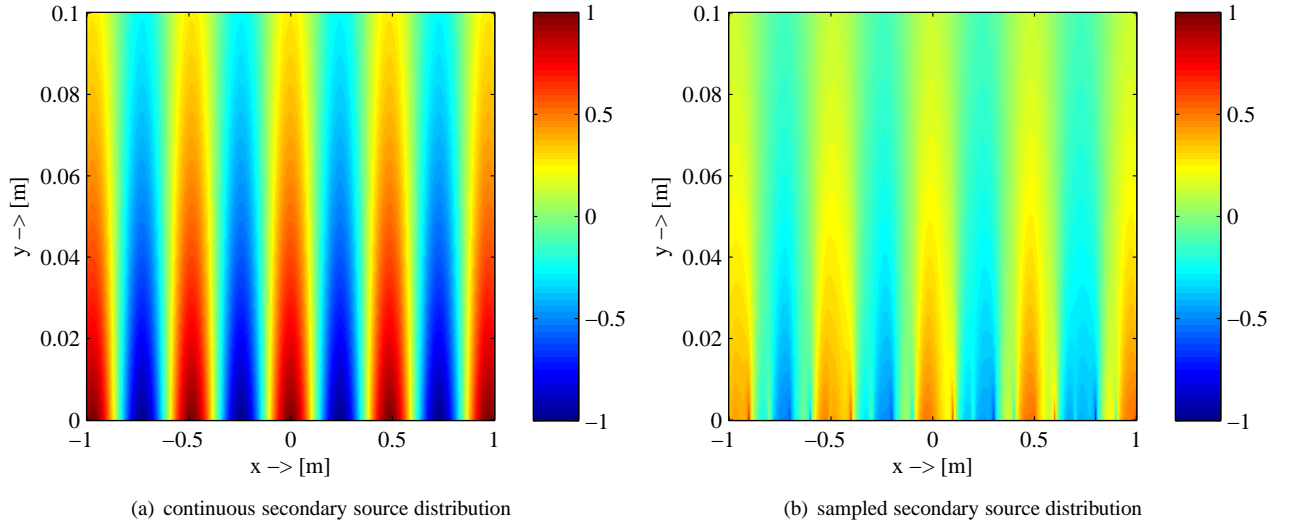


**Fig. 5:** Comparison of the evanescent part of the wave field reproduced by a continuous and sampled secondary source distribution ( $\Delta x = 10$  cm) for the reproduction of a plane wave with frequency  $f = 1000$  Hz and incidence angle  $\alpha_{pw} = 45^\circ$ .

spectrum of the reproduced wave field as

$$\tilde{P}_{tr}(\mathbf{k}, \omega) = -\frac{1}{2\pi} \underbrace{(\tilde{w}(k_x) *_{k_x} \tilde{D}(k_x, \omega))}_{\tilde{D}_{tr}(k_x, \omega)} \tilde{G}(\mathbf{k}, \omega), \quad (19)$$

where  $*_{k_x}$  denotes convolution with respect to the spatial frequency  $k_x$ -variable. A secondary source distribution with finite length  $L$  can be modeled by a rectangular window. In this case the window function  $w(x_0)$  is given by the rect-function [5]

$$\text{rect}\left(\frac{x}{L}\right) = \begin{cases} 1 & , \text{ if } |x| \leq \frac{L}{2}, \\ 0 & , \text{ otherwise.} \end{cases} \quad (20)$$

The spatial Fourier transformation of  $\text{rect}(\frac{x}{L})$  with respect to the  $x$ -variable can be computed as

$$\mathcal{F}_x\{\text{rect}\left(\frac{x}{L}\right)\} = |L| \frac{\sin(\frac{k_x L}{2})}{\frac{k_x L}{2}} = |L| \text{sinc}\left(\frac{k_x L}{2}\right). \quad (21)$$

Other window functions can also be applied to limit truncation effects caused by the hard truncation in space [1]. We will outline the formulation of the reproduced spectrum at the example of the rect-window in the following. However, the same principles apply also to other window functions. Applying the procedure outlined in [3] to

the case of a truncated sampled linear array derives the reproduced wave field as follows

$$\begin{aligned} \tilde{P}_{S, tr, pw}(\mathbf{k}, \omega) = & \pi \frac{\omega}{c} \sin \alpha_{pw} |L| \sum_{\eta=-\infty}^{\infty} \text{sinc}\left(\frac{L}{2}\left(k_x - \frac{2\pi}{\Delta x} \eta - \frac{\omega}{c} \cos \alpha_{pw}\right)\right) \times \\ & \times \left( \frac{1}{k} \delta\left(\sqrt{k_x^2 + k_y^2} - \frac{\omega}{c}\right) + j \frac{1}{k_x^2 + k_y^2 - \left(\frac{\omega}{c}\right)^2} \right). \quad (22) \end{aligned}$$

Hence, the Dirac lines in Fig. 4 will be replaced by shifted sinc-functions at the positions of the Dirac lines. The spectrum of the reproduced propagating wave field is derived by applying the sifting property of the circular Dirac line  $\delta(\sqrt{k_x^2 + k_y^2} - \frac{\omega}{c})$  in Eq. (22) to the shifted sinc-functions. The result is a circular Dirac function which is weighted in the  $k_x$ -direction by the shifted sinc-functions. For  $\eta = 0$  (continuous case) this will result in the reproduction of a plane wave superimposed by truncation artifacts. For a sampled secondary source distribution, the repetitions of the sinc functions at  $\frac{2\pi}{\Delta x} \eta$  will also interfere with the baseband, since the sinc-function has contributions at all spatial frequencies  $k_x$ . As a consequence, no exact anti-aliasing conditions can be given for the truncated linear array. However, an aliasing-to-signal (ASR) ratio [4] could be used to characterize the

aliasing contributions. However, the ASR will depend on the choice of the particular window function  $w(x_0)$  used for truncation. Here might be some potential for optimization with respect to aliasing artifacts of finite length linear arrays. The same procedure as outlined above can also be applied to the imaginary valued part of the spectrum.

#### 4. POINT SOURCES AS SECONDARY SOURCES

Most practical implementations of WFS systems use closed loudspeakers (point sources) as secondary sources for the reproduction in a plane. The consequences of this secondary source mismatch have been pointed out in Section 2.2. This section will derive the reproduced spectrum and will outline its interpretation.

The reproduced spectrum  $\tilde{P}_{pw}(\mathbf{k}, \omega)$  is derived by introducing the spectrum of the three-dimensional Green's function  $\tilde{G}_{3D}(\mathbf{k}, \omega)$  and the driving function  $\tilde{D}(k_x, \omega)$  into Eq. (7). Applying the procedure shown in Section 3.1 yields

$$\tilde{P}_{pw}(\mathbf{k}, \omega) = \frac{j\omega}{c} \sin \alpha_{pw} \times \delta(k_x - \frac{\omega}{c} \cos \alpha_{pw}) \frac{1}{\sqrt{k_x^2 + k_y^2 - (\frac{\omega}{c})^2}}, \quad (23)$$

where the spectrum of the Green's function  $\tilde{G}_{3D}(\mathbf{k}, \omega)$  given in [3] was used. A detailed analysis of the reproduced wave field for point sources as secondary source could be performed, similar as for the secondary line sources, by computing the inverse spatial Fourier transformation of the real and imaginary valued parts of the reproduced wave field  $\tilde{P}_{pw}(\mathbf{k}, \omega)$ . However, the detailed solution and its implications go beyond the scope of this paper and is topic of ongoing research. First results indicate that no near-field artifacts (evanescent plane waves) are reproduced for point sources as secondary sources. Interestingly this finding seems to be in conjunction with other research results in the area of numerical simulation of sound propagation [13].

A first approximation of the reproduced field can be gained from Eq. (4) for  $k|\mathbf{x} - \mathbf{x}_0| \gg 1$ , hence for a reasonable distance from the array (far-field) or high frequencies. The reproduced propagating part will not have equal amplitude throughout the entire listening area, it will be superimposed by a decaying amplitude over distance to the array.

#### 5. SUMMARY AND CONCLUSIONS

This paper presented a detailed analysis of the sound field reproduced by a linear secondary line source distribution. The analysis was based on a spatio-temporal spectral analysis of the reproduced wave field. Investigation of the spectral components revealed that beside the desired wave field also evanescent contributions are emitted by the secondary sources. In the continuous case an evanescent plane wave was reproduced with similar parameters as the desired wave field, but with decaying amplitude perpendicular to the array axis. Due to this amplitude decay the evanescent wave will only have influence in the vicinity (near-field) of the secondary sources. It was further shown that for a sampled secondary source distribution no anti-aliasing condition can be given for this part since aliasing is always present in the reproduced evanescent plane wave. This result is quite remarkable since this is not the case for the propagating part. The analysis of the reproduced wave field was complemented by quantitatively considering truncation of the array and indicating the consequences of using point sources as secondary sources. Most WFS systems are built using closed loudspeakers (point sources) as secondary sources. However, the use of (truncated) line arrays, where several closed loudspeakers are used for one secondary source, has proven to be a promising concept with several benefits [14, 15].

The results presented in this paper together with the previous publications [3, 4] provide the theoretical link between the wave field reproduced by a continuous and a sampled (loudspeaker array) secondary source distributions used for sound reproduction. The derived results can be generalized straightforwardly to other massive multichannel sound reproduction systems (e. g. higher-order Ambisonics) by modifying the driving function accordingly and performing the steps shown in this paper. Besides sound reproduction only, WFS has also been applied to active control applications like active noise control (ANC) or active listening room compensation. The presented near-field effects of linear arrays will limit the performance of such applications in the vicinity of the loudspeaker array. The presented results allow to quantify the performance degradations in practical situations by considering sampling and truncation.

However, an open question still is the audibility of the derived near-field effects. The physically based analysis presented here revealed their evanescent nature. The question remains if evanescent plane waves are audible to humans, and if this is the case, how they are perceived

by them. The authors did not find conclusive literature on the topic to finally answer this question.

Further research topics and directions are the exact analysis of near-field effects for point sources as secondary sources, the use of more sophisticated models for the secondary sources (e. g. a piston radiator model [16]) and experimental validation of the results.

The results derived in this paper have some indications on the theoretical background of sound reproduction systems that are essentially based on the Kirchhoff-Helmholtz integral. It is often assumed that it is sufficient to use the directional gradient of the virtual source on the boundary of the listening area as driving signal in order to perfectly reproduce the wave field of the virtual source inside the listening area. This paper revealed a potentially undesired additional near-field effect for linear arrays. There is strong evidence that these results hold also for arbitrary secondary source contours.

## 6. REFERENCES

- [1] E.W. Start. *Direct Sound Enhancement by Wave Field Synthesis*. PhD thesis, Delft University of Technology, 1997.
- [2] A.J. Berkhout, D. de Vries, and P. Vogel. Acoustic control by wave field synthesis. *Journal of the Acoustic Society of America*, 93(5):2764–2778, May 1993.
- [3] S. Spors. Spatial aliasing artifacts produced by linear loudspeaker arrays used for wave field synthesis. In *Second IEEE-EURASIP International Symposium on Control, Communications, and Signal Processing*, Marrakech, Morocco, March 2006.
- [4] S. Spors and R. Rabenstein. Spatial aliasing artifacts produced by linear and circular loudspeaker arrays used for wave field synthesis. In *120th AES Convention*, Paris, France, May 2006. Audio Engineering Society (AES).
- [5] B. Girod, R. Rabenstein, and A. Stenger. *Signals and Systems*. J.Wiley & Sons, 2001.
- [6] S. Spors. *Active Listening Room Compensation for Spatial Sound Reproduction Systems*. PhD thesis, University of Erlangen-Nuremberg, 2006.
- [7] R. Rabenstein and S. Spors. Wave field synthesis techniques for spatial sound reproduction. In E.Haensler and G.Schmidt, editors, *Topics in Acoustic Echo and Noise Control*, chapter 13, pages 517–545. Springer, 2006.
- [8] E.G. Williams. *Fourier Acoustics: Sound Radiation and Nearfield Acoustical Holography*. Academic Press, 1999.
- [9] M. Abramowitz and I.A. Stegun. *Handbook of Mathematical Functions*. Dover Publications, 1972.
- [10] S. Spors, M. Renk, and R. Rabenstein. Limiting effects of active room compensation using wave field synthesis. In *118th AES Convention*, Barcelona, Spain, May 2005. Audio Engineering Society (AES).
- [11] J.-J. Sonke, D. de Vries, and J. Labeeuw. Variable acoustics by wave field synthesis: A closer look at amplitude effects. In *104th AES Convention*, Amsterdam, Netherlands, May 1998. Audio Engineering Society (AES).
- [12] I.S. Gradshteyn and I.M. Ryzhik. *Tables of Integrals, Series, and Products*. Academic Press, 2000.
- [13] E.M. Stein and R. Shakarchi. *Fourier Analysis: An Introduction*. Princeton University Press, 2003.
- [14] B. Pueo, J. Escolano, S. Bleda, and J.J. Lopez. An approach for wave field synthesis high power applications. In *118th AES Convention*, Barcelona, Spain, May 2005. Audio Engineering Society (AES).
- [15] E. Hulsebos. *Auralization using Wave Field Synthesis*. PhD thesis, Delft University of Technology, 2004.
- [16] L.E. Kinsler, A.R. Frey, A.B. Coppens, and J.V. Sanders. *Fundamentals of Acoustics, 4th Edition*. Wiley, 2000.